Layout: T1 Standard Unicode | Book ID: 314356_1_En | Book ISBN: 978-3-319-21649-2
Chapter No.: 11 | Date: 24-10-2015 Time: 10:33 am | Page: 1/25

Chapter 11
Glaciers and Monsoon Systems

Bodo Bookhagen

Abstract This chapter will analyze the impact of monsoon systems on glaciers. Most of the tropical glaciers in the Andes and Himalayas vary greatly in time and space, and are heavily influenced by their corresponding monsoon systems. This chapter will review climatic boundary conditions and provide a regional assessment of glacial changes in monsoonal systems with focuses on the central Andes and Himalayas.

Keywords Andes · Himalayas · High Mountain Asia · Atmospheric lapse rate · Snow water equivalent · Runoff · Glacial contribution

11.1 Glaciers and Global Monsoon Systems

Glaciers around the world are rapidly shrinking, especially in low-latitude regions (Baraer et al. 2012; Bolch et al. 2011, 2012; Bradley et al. 2006; Hanshaw and Bookhagen 2014; Huss 2012; Kaser et al. 2006; Oerlemans 2005; Price and Weingartner 2012; Vaughan et al. 2013; Vuille et al. 2008). Glaciers are an important source of clean water and provide a significant portion of the annual hydrologic budget in some regions (Archer and Fowler 2004; Huss et al. 2008; Kaser et al. 2010; Radic and Hock 2011; Vaughan et al. 2013; Viviroli and Weingartner 2004). Especially in the tropical Andes, glacial-melt contribution is important (Kaser et al. 2010; Vuille et al. 2008); other tropical and low-latitude regions with mountain ranges obtain their runoff from transiently stored waters in the form of snow and ice (Barnett et al. 2005; Bookhagen and Burbank 2010; Kaser et al. 2010; Viviroli and Weingartner 2004). However, the contribution of glacial runoff is difficult to determine and varies from year to year. Remote-sensing studies

B. Bookhagen (✉)
Institute of Earth and Environmental Science, University of Potsdam,
Karl-Liebknecht-Str. 24/25, 14467 Potsdam-Golm, Germany
e-mail: Bodo.Bookhagen@uni-potsdam.de

L.M.V. de Carvalho and C. Jones (eds.), *The Monsoons and Climate Change*,
Springer Climate, DOI 10.1007/978-3-319-21650-8_11

Layout: T1 Standard Unicode Book ID: 314356_1_En Book ISBN: 978-3-319-21649-2
Chapter No.: 11 Date: 24-10-2015 Time: 10:33 am Page: 2/25

can help to assess general trends in glacial areas, elevation changes, and velocities, but in situ field work adds crucially important measurements unavailable at the scale of the most remotely sensed datasets (Finger et al. 2012; Hanshaw and Bookhagen 2014; Huggel et al. 2002; Paul et al. 2004; Quincey et al. 2007; Scherler et al. 2011a, b).

From a geographic perspective, glaciers in the tropics and low-latitude regions are limited to high-elevation regions where temperatures are low enough to maintain year-round ice. The areas that this chapter will focus on are the Andes of South America and the Himalayas in eastern Asia (Fig. 11.1); both areas are glacierized to different degrees because of their varying topographic and climatic boundary conditions.

Here, we loosely define global monsoon regions as the areas where the grid-cell summer-minus-winter precipitation rate exceeds 2.5 mm/day and the local summer precipitation exceeds 55 % of the annual total (Wang and Fan 1999) (Fig. 11.1).

While glaciers are important for water resources in some tropical regions, the seasonal snow cover may provide an equally important contribution to annual runoff (Bookhagen and Burbank 2010; Viviroli and Weingartner 2004). For example, river systems in the western and northwestern Himalayas, such as the Indus, derive more than 50 % of their annual runoff from snow-melt waters (Archer and Fowler 2004; Bookhagen and Burbank 2010; Immerzeel et al. 2009), but only a small percentage of runoff is derived from glacial-melt waters (Jeelani et al. 2012). There is no significant snow cover in the central Andes, but south of 30°S, the Andes have a persistent seasonal snow cover (Figs. 11.2 and 11.4), but this is

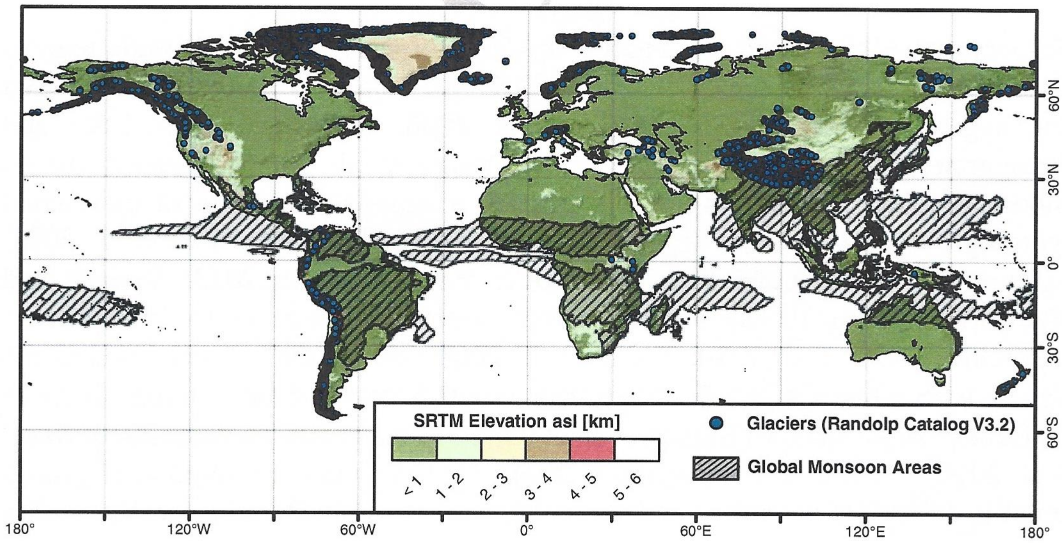

Fig. 11.1 Global distribution of glaciers using the Randolph Catalog (V3.2—*blue dots*) (Arendt et al. 2012), shaded-relief topography (SRTM) (Farr et al. 2007), and TRMM 3B42V7-based monsoonal areas (*gray-hatched areas*) (Huffman et al. 2007). Global monsoon domains are approximated by the approach of B. Wang and Fan (1999), where the grid-cell summer-minus-winter precipitation rate exceeds 2.5 mm/day and the local summer precipitation exceeds 55 % of the annual total

Layout: T1 Standard Unicode | Book ID: 314356_1_En | Book ISBN: 978-3-319-21649-2
Chapter No.: 11 | Date: 24-10-2015 | Time: 10:33 am | Page: 3/25

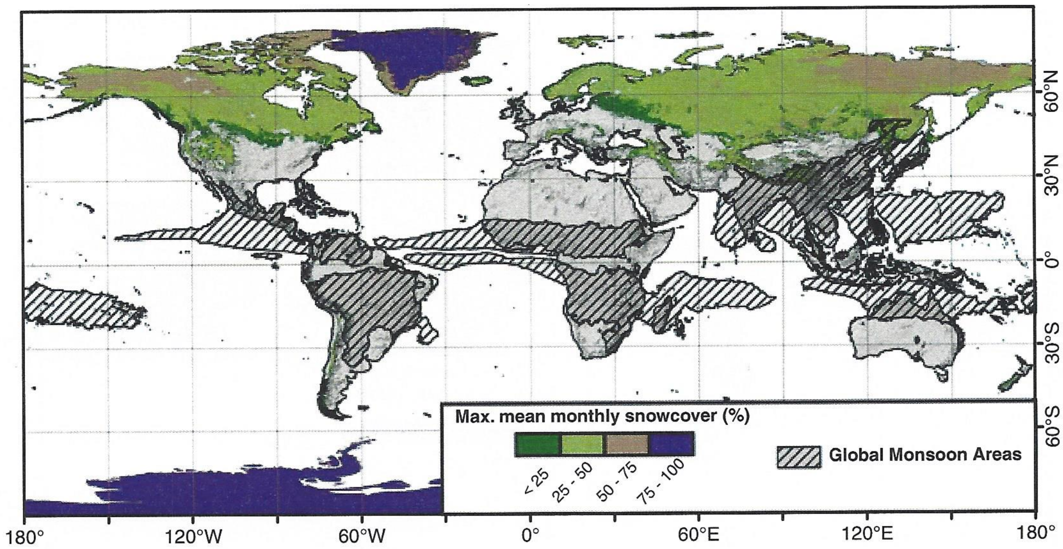

Fig. 11.2 Maximum annual snow cover extent based on MODIS product MOD10C1.005 (Hall et al. 2006) from February 2000 until April 2014. *Hashed areas* indicate global-monsoon areas (cf. Fig. 11.1). Note the low snow cover for most monsoonal areas, except in the Himalayas

Hatched

outside the South American Monsoon domain. The Himalayas have a seasonal snow cover, especially in their west and northwest, at elevations above 4 or 5 km (Fig. 11.2). AQ1

Snow-cover measurements based on satellite imagery only indicate areal extent, but not snow volume or snow amount. For example, a thin, persistent snow cover may have the same signal as a thick, seasonal cover, but their water equivalents differ significantly. Hence, snow water equivalent (SWE) measurements give a better estimate for the amount of water stored in high elevation areas. However, remote-sensing measurements of SWE do not have high spatial resolution and are hampered by technical difficulties (Pulliainen and Hallikainen 2001; Tait 1998; Tedesco et al. 2004b). A compilation of annual SWE for ~10 years—from 2002 to 2011—shows high SWE amounts for the global monsoonal domain only in the Himalayas (Fig. 11.3). The southern Andes show significant seasonally stored SWE as well, but are not part of the global monsoon domain.

The IPCC's Fourth Assessment identifies snowmelt as a key component of the hydrology and climate for High Mountain Asia (HMA)—roughly defined as the area from the Tien Shan in the north, down to the Himalayas in the south, and from the Pamir in the west to the edge of the Tibetan Plateau in the east (Jacob et al. 2012; Lemke et al. 2007). The time lag between seasonal snowfall and snowmelt sustains runoff during the drier summer months. A warmer climate could change the timing of melt and the volume of the snowpack, and would have significant consequences for water resources and power generation, particularly in year-round water provisioning. Among the world's snow-dominated regions, the western Himalayas and central Asia are particularly susceptible to changes in the timing of snowmelt, as reservoir capacity is currently not sufficient to buffer large seasonal shifts in the hydrograph (Barnett et al. 2005). Similarly, the IPCC's Fifth Assessment report

Layout: T1 Standard Unicode | Book ID: 314356_1_En | Book ISBN: 978-3-319-21649-2
Chapter No.: 11 | Date: 24-10-2015 Time: 10:33 am | Page: 4/25

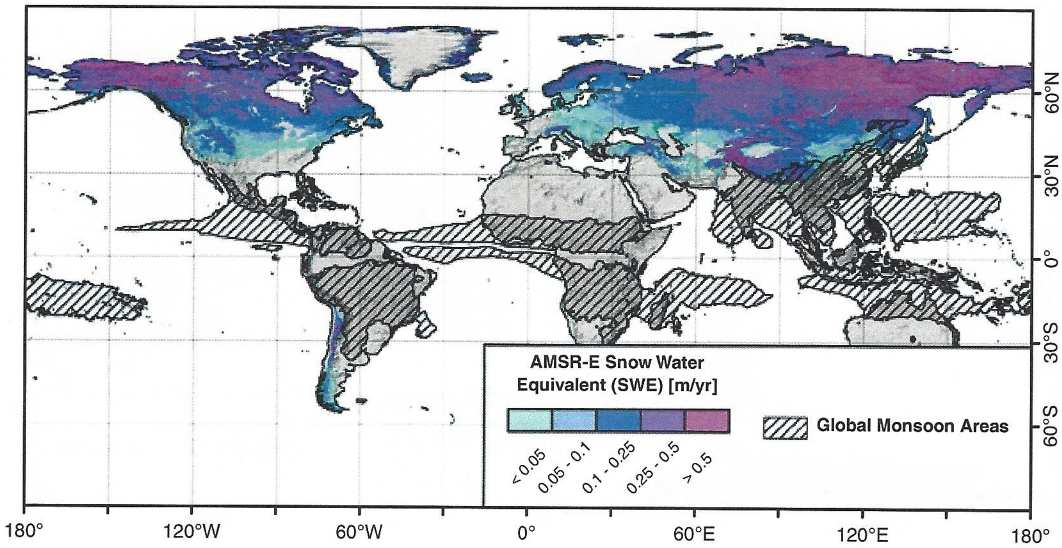

Fig. 11.3 Annual snow water equivalent (SWE) based on passive microwave data (AMSR-E) (Tedesco et al. 2004a) from June 2002 to Oct 2011. SWE is generally low in monsoon-dominated areas (cf. Fig. 11.1), except in High Mountain Asia (HMA)

released in the fall of 2013 makes clear regional distinction in societal impacts due to transiently stored moisture in the form of snow, ice, and permafrost (IPCC 2013).

Taken together, many large cities and densely populated areas in the Andes and Himalayas are located above 2,000 m elevation and depend almost entirely on high altitude water stored in snowpack and glaciers to complement scarce rainfall during the dry season. The increase in glacial melting leads to higher glacial melt water fluxes, but much of the water loss is no longer seasonally restored. The long-term consequences of this are that dry-season runoff will be significantly reduced over the coming decades. While wet season runoff may be higher for the first few decades—due to increased melting—it will decline when the glaciers start to adjust to their new equilibriums. Importantly, mean annual runoff may not change very much, but when water is most needed during the dry season to support agriculture and hydropower generation, water availability will be significantly reduced.

In the tropical areas influenced by the monsoon, temperature remains nearly constant throughout the year, but the hydrological cycle typically has pronounced wet and dry phases. For that reason, the mass and surface energy balance of tropical glaciers are very different than mid- or high-latitude glaciers (Kaser 2001; Vuille et al. 2008; Wagnon et al. 1999). At mid- or high latitudes, winter is the accumulation and summer the ablation season, but ablation and accumulation occur year-round on tropical glaciers. Because of the relatively stable year-round temperature regime, melting occurs mainly in the ablation zone below the snow line altitude, and accumulation is mostly restricted to regions above the snow-rain line, which often remains at a constant altitude throughout the year (Vuille et al. 2008). Field studies and field measurements are rare throughout the tropical regions due to the high altitude of the glaciers, but the few existing studies reveal that the largest mass loss and gain occurs during wet seasons (Francou et al. 2003). In the South

American Monsoon domain, inter-annual glacial variations are also controlled by the El Niño-Southern Oscillation (ENSO) phenomenon, which dictates moisture transport and controls regional temperature. Positive ENSO cycles often result in strongly negative glacial mass balances (melting) due to reduced moisture transport into the central Andes (Bookhagen and Strecker 2010). In contrast, moisture transport during negative ENSO cycles is often increased and results in balanced or slightly positive mass balances in glaciers in the north-central and central Andes (Francou et al. 2003; Vuille et al. 2008; Wagnon et al. 2001).

This section summarizes some of the recent findings in cryospheric sciences, regional retreat rates, climatic trends, and their impact on the downstream society. In a second step, I will link global glacial distributions to monsoon domains and will focus on the South American Andes and the Himalayas in eastern Asia.

11.2 Datasets and Methods

The analysis and synthesis presented in this paper relies on several field and remote-sensing datasets. I rely on high-spatial resolution remote sensing data, because most climatic re-analysis datasets do not have the spatial resolution necessary to capture the steep climatic and topographic gradients of large mountain ranges.

Glacial extents were derived from the Randolph Glacier Inventory (RGI), a community-based dataset of global glacier outlines (Version 3.2) (Arendt et al. 2012) (Fig. 11.1). These data are referred to as RGI V3.2. Additional glacial outlines were taken from Hanshaw and Bookhagen (2014) for the central Andes.

Rainfall data were based on the Tropical Rainfall Measurement Mission (TRMM) product 3B42 (Boers et al. 2013; Bookhagen 2010; Bookhagen and Strecker 2010; Huffman et al. 2007). This product has a 3-h temporal resolution (data were aggregated to daily time steps) and a spatial resolution of 0.25° × 0.25° (about 25 × 25 km^2) with an observational range from 1998 to 2014. In addition, high-spatial resolution TRMM 2B31 data were used to decipher orographic rainfall barriers. These data are based on the raw orbital observations that have been interpolated to regularly-spaced 90-m grids (Bookhagen and Burbank 2006, 2010; Bookhagen and Strecker 2008, 2012). A study comparing TRMM 3B42 with various other precipitation datasets for South America indicates good agreement between station and remotely sensed data at large spatial scales (Carvalho et al. 2012). A comparison of station data and gridded rainfall data for the Himalayas indicates that TRMM 3B42 and TRMM 2B31 perform reasonably well (Andermann et al. 2011).

Snow cover data were derived from the MODIS (Moderate Resolution Imaging Spectroradiometer) product MOD10C1 daily dataset with 0.05° × 0.05° (~5 × 5 km^2) spatial resolution (Hall et al. 2006). Data were aggregated to monthly or seasonal time steps where needed. Data ranged between March 2001 and April 2014.

Layout: T1 Standard Unicode | Book ID: 314356_1_En | Book ISBN: 978-3-319-21649-2
Chapter No.: 11 | Date: 24-10-2015 | Time: 10:33 am | Page: 6/25

Land Surface Temperature data were derived from the MODIS product MOD11C1 daily dataset with 0.05° × 0.05° spatial resolution (Wan 2008; Wan and Dozier 1996). Here, we rely on the nighttime data because they provide more accurate surface-temperature measurements (Bookhagen and Burbank 2010; Wang et al. 2008). Data were aggregated to monthly values where needed.

Snow water equivalent (SWE) is based on passive microwave measurements onboard the AMSR-E (Advanced Microwave Scanning Radiometer—EOS) platform (Pulliainen and Hallikainen 2001; Tait 1998; Tedesco et al. 2004b). Daily data with a spatial resolution of 0.25° × 0.25° were generated between May 2002 and Oct 2011.

I have ~~The author has~~ used the centroids of glacial outline polygons from RGI V3.2 for display purposes (e.g., Figs. 11.1 and 11.4), and has used the polygon extents to calculate topographic and climatic statistics from various datasets (e.g., Figs. 11.5 and 11.10).

Along-latitude (Fig. 11.5) and along-longitude (Figs. 11.6 and 11.10), profiles were generated for each row or column of data, respectively—that is, the along-latitude profile for the Andes was generated by first projecting all data to an equal-area grid with the same spatial resolution using bilinear resampling. Secondly, row-wise statistical measurements (average, minimum, maximum) were generated for elevations >500 m asl, which correspond to the mountainous Andes and exclude low-lying areas. Finally, these data were smoothed with a 5-km running-average filter along the profile direction.

11.3 Glaciers in the Andes and the South American Monsoon System (SAMS)

11.3.1 Climatic Background

The South American Monsoon System (SAMS) is an important feature of the global monsoon domain (e.g., Kitoh et al. 2013) and is characterized by highly seasonal features. For an in-depth review, refer to Carvalho et al. (2011b); Marengo et al. (2012); Vera et al. (2006). A comprehensive description of the SAMS is found in Chap. 6 of this book.

In short, low-level moisture transport from the tropical Atlantic onto the South American continent is driven by trade winds initiated near the Intertropical Convergence Zone (ITCZ), in combination with differential heating between ocean and land during the monsoon season (December–January–February, DJF) (Marengo et al. 2012; Vera et al. 2006). An integral part, and the most distinctive feature of the SAMS, is the South Atlantic Convergence Zone (SACZ), which is characterized by a convective band of precipitation extending southeastward from the central Amazon Basin (Carvalho et al. 2002; Jones and Carvalho 2002). The SACZ exhibits a dipole-like pattern with strengthened precipitation in the SACZ when precipitation in southeast South America (SESA) is reduced, and vice versa

Layout: T1 Standard Unicode Book ID: 314356_1_En Book ISBN: 978-3-319-21649-2
Chapter No.: 11 Date: 24-10-2015 Time: 10:33 am Page: 7/25

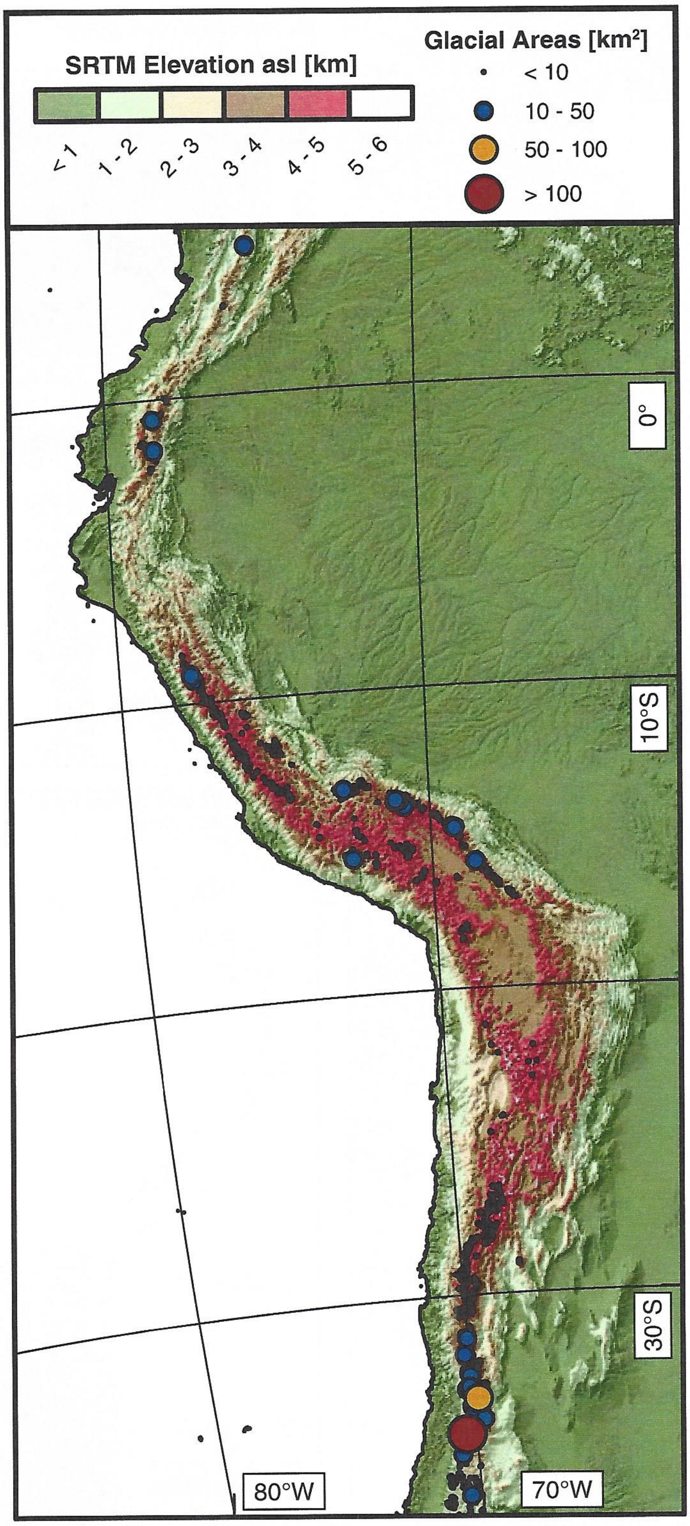

Fig. 11.4 Topography and glacial sizes based on RGIV3.2 (Arendt et al. 2012) for South America. The large majority of glaciers in the northern and central Andes are <10 km^2 (cf. glacial sizes for the Himalayas in Fig. 11.8). Outside the monsoon-influenced region south of 30°S, larger glaciers exist due to higher moisture influx

(e.g., Carvalho et al. 2004; Marengo et al. 2012; Vera et al. 2006). The low-level flow from the Amazon basin westward in the form of the South American Low-Level Jet (SALLJ) is deflected southward by the Andes (Marengo et al. 2012). When the moisture-laden clouds are orographically lifted, they result in a prominent

Layout: T1 Standard Unicode | Book ID: 314356_1_En | Book ISBN: 978-3-319-21649-2
Chapter No.: 11 | Date: 24-10-2015 | Time: 10:33 am | Page: 8/25

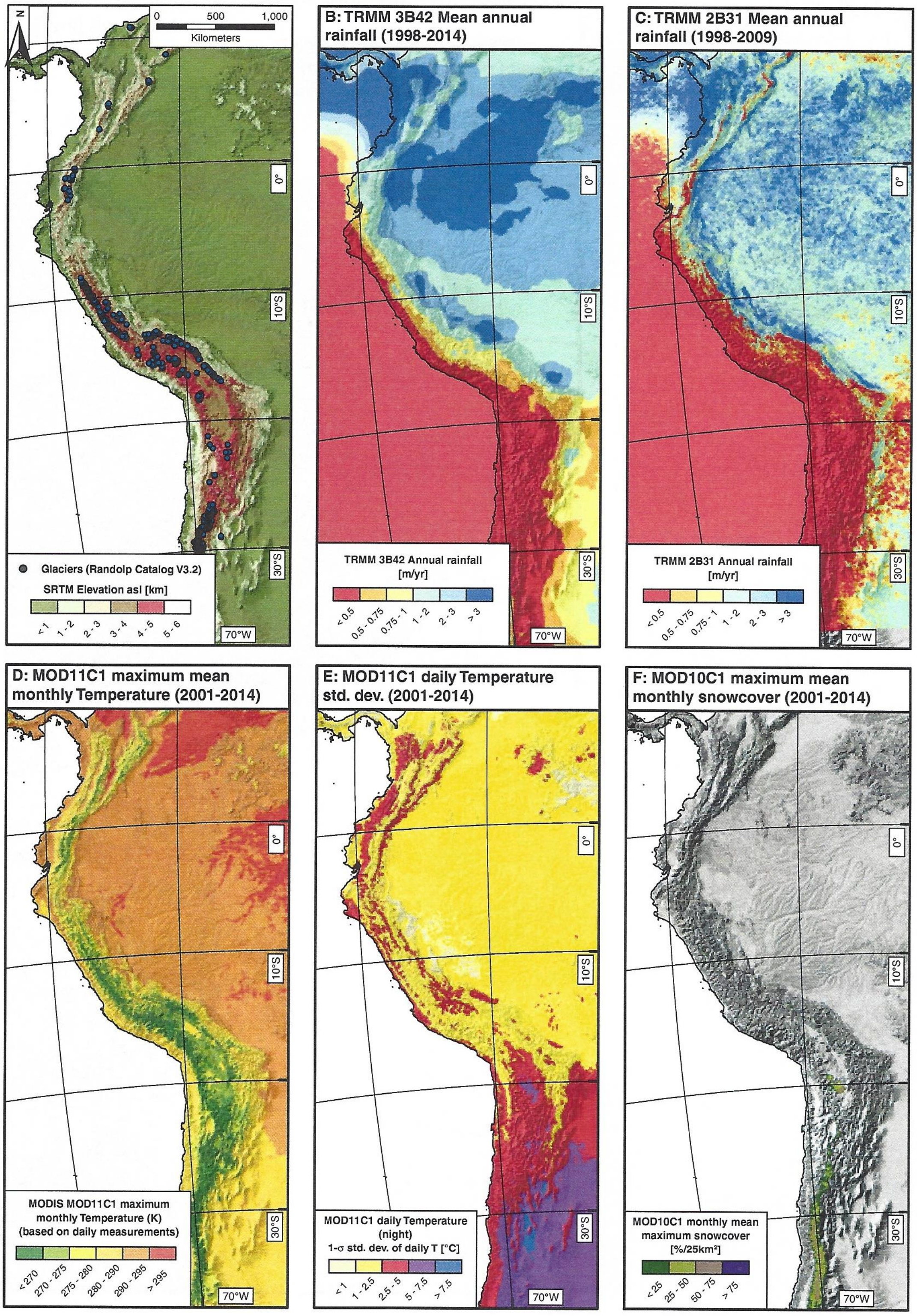

◀ **Fig. 11.5** **a** Dataset compilation for South America. *Top left panel* shows topography and glacier location based on RGI V3.2 (Arendt et al. 2012). **b** Mean annual TRMM 3B42 rainfall (spatial resolution: $\sim 25 \times 25$ km^2 and 3-h temporal resolution) (Boers et al. 2013; Bookhagen and Strecker 2010; Huffman et al. 2007). **c** Mean annual rainfall based on high-spatial resolution TRMM 2B31 data (Bookhagen and Burbank 2006, 2010; Bookhagen and Strecker 2008). Note the overall similarity between TRMM 3B42 and 2B31, but the generally more pronounced orographic rainfall peak along the eastern Andes due to the higher spatial resolution of product 2B31. **d** MODIS MOD11C1 maximum mean monthly temperature based on daily data from March 2001 to April 2014 collected during nighttime conditions (Wan 2008). Note the temperature gradient between the high-elevation Andes and the low-elevation Amazon plains. **e** 1-sigma standard deviation of daily temperatures from March 2001 to April 2014. Note the low variability in the tropical regions, including the tropical Andes. However, in the subtropical regions at ~27°S, nighttime temperature variability exceeds 7.5 and 10 °C. **f** MODIS MOD10C1 maximum mean monthly snow cover based on daily data from March 2001 to April 2014 (Hall et al. 2006). There is no significant snow cover in the central Andes in the tropical regions, but in the subtropical southern Andes, snow cover becomes more dominant

orographic rainfall peak along the eastern Andean mountain front (Bookhagen and Strecker 2008) (Fig. 11.4c). Rainfall peaks at the mountain front at elevations of ~1 km; rainfall at higher elevations, for example above 3 km, is greatly reduced (Boers et al. 2013; Bookhagen and Strecker 2008, 2012). The steep topographic gradient results in a significant climatic gradient from east to west across the eastern Andes: the frontal areas are moist, tropical climates with mean annual rainfall >4 m/year (Bookhagen and Strecker 2008) and dense vegetation cover. The higher elevation areas—only 100 km westwards—are semi-arid to arid (<0.5 m/year), with little to no vegetation cover. It is this steep climatic gradient that defines mountain climate and makes this region very vulnerable to climate shifts (Baraer et al. 2012; Barnett et al. 2005; Bradley et al. 2006).

The tropical Andes contain more than 99 % of the world's tropical glaciers: Peru 71 %, Bolivia 20 %, Ecuador 4 %, and Colombia-Venezuela 4 % (Kaser 1999) (Fig. 11.4). In most north-central Andean regions, glaciers cover the highest peaks, which are often volcanoes in the northern Andes (Figs. 11.1 and 11.5). Several mountain peaks in the central and south-central Andes are presently too dry to maintain glaciers, but extensive evidence suggests past glaciation on these peaks (Abbott et al. 2003; Haselton et al. 2002; Thompson et al. 2003). The runoff generated from some of these tropical glaciers are an integral part of the hydrologic cycle in the northern and north-central Andes, especially in Peru (e.g., Kaser et al. 2010). Furthermore, melt waters from these glaciers provide resources not only for drinking water and hydropower generation, but also for agriculture and recreation (Buytaert et al. 2006, 2011; Buytaert and De Bievre 2012).

11.3.2 Glacial Retreat Rates and Trends

Glacial retreat in the tropical Andes over the last three decades is unprecedented since the maximum extension of the Little Ice Age (LIA, mid-seventeenth to early eighteenth centuries) (Rabatel et al. 2013). Venezuela has the northernmost tropical

Layout: T1 Standard Unicode | Book ID: 314356_1_En | Book ISBN: 978-3-319-21649-2
Chapter No.: 11 | Date: 24-10-2015 Time: 10:33 am | Page: 10/25

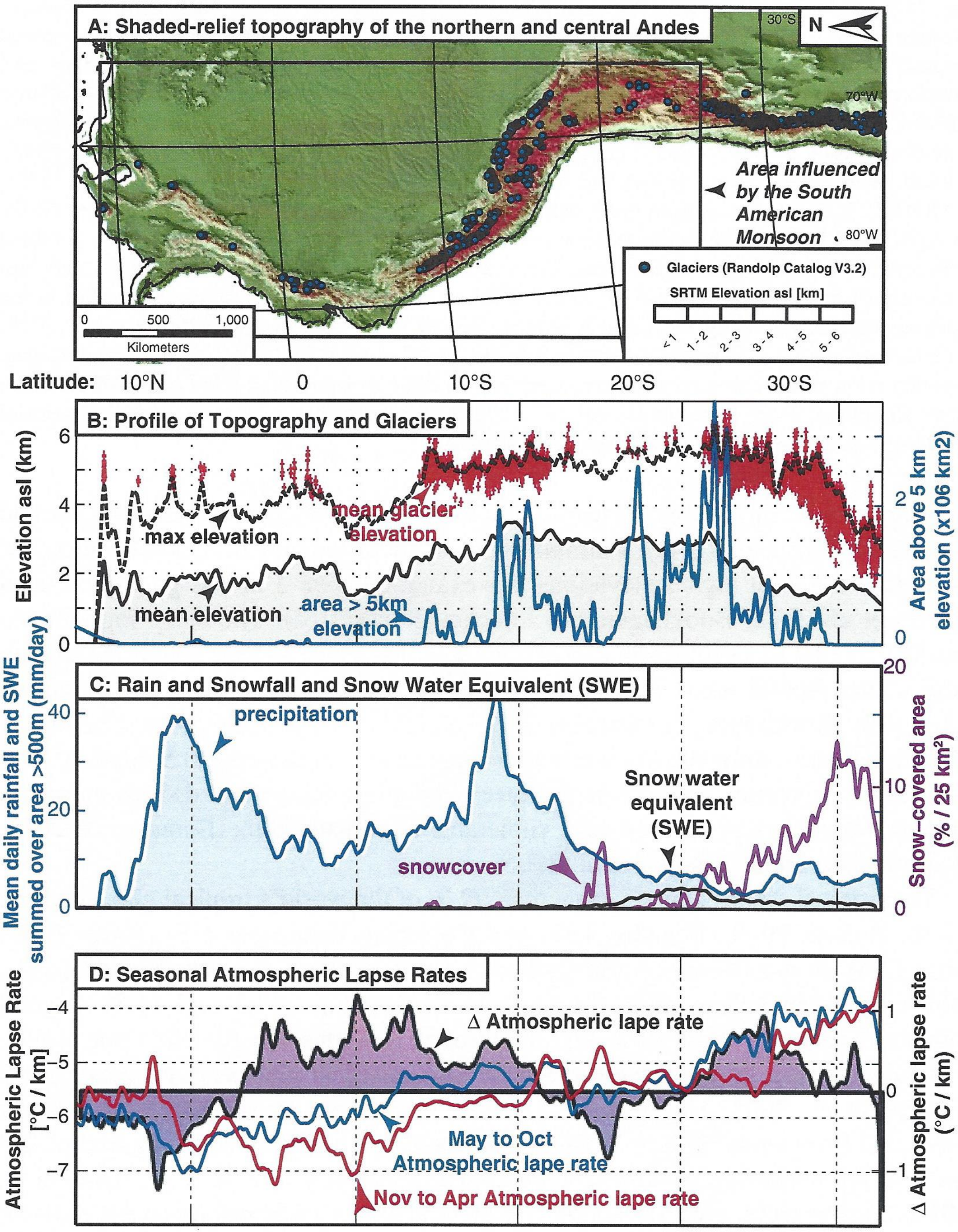

◀ **Fig. 11.6** Topographic, climatic, and glacial distribution through South America. **a** Shaded-relief topography of the northern and central Andes shows glacier locations (Arendt et al. 2012). *Black box* outlines the area influenced by the South American Monsoon System (cf. *hashed areas* in Fig. 11.1). **b** Shows topographic profile from North to South along the Andes orogen for elevations above 500 m asl (i.e., grid cells from the Amazon Basin and other low-elevation areas are excluded). The maximum elevation (*dashed line*) denotes peaks. Most of the peaks near the Equator are volcanoes that are covered by small glaciers. Note that the heavily glacierized areas in the southern Andes are not part of the monsoon domain (south of ~28°S). **c** The heavily glaciated Cordillera Oriental in Peru (~10°S) is characterized by high monsoonal precipitation, but low snow cover. Throughout the tropical Andes, there is no persistent snow cover and only very little snow-water equivalent (SWE) amounts. Only at the southern end of the monsoon domain, widespread snow cover and SWE become more dominant. SWE and precipitation are scaled similarly and show the daily water amount for the area above 500 m elevation. This can be converted to annual amounts by multiplying with 365. **d** Atmospheric lapse rate (°C/km) for the austral summer (November–April) and winter (May–October) is between −7 and −5 °C/km for the northern and central Andes, but increases to >−5 °C/km to the south of the monsoon domain. Note that seasonal lapse rate differences in the central Andes can exceed 1 °C/km

glacier (Figs. 11.1 and 11.4), but has lost more than 95 % of its glacier-covered area since the 1950s (Vuille et al. 2008). Peru contains the largest amount of all tropical glaciers in the low latitudes, and most of these glaciers are located in the monsoon-dominated Cordillera Occidental and Oriental (Figs. 11.1 and 11.4) (Arendt et al. 2012; Rabatel et al. 2013; Vuille et al. 2008). Similarly, glaciers in the Cordillera Vilcanota and the Quelccaya Ice Cap area in the northern central Andes in Peru have retreated with rates of 3.99 ± 1.15 km^2 $year^{-1}$ (Cordillera Vilcanota) and 0.57 ± 0.19 km^2 $year^{-1}$ (Quelccaya Ice Cap) (Hanshaw and Bookhagen 2014). Importantly, glacial retreat has accelerated between the decades of 1988–1999 and 2000–2010 by 13 % (Hanshaw and Bookhagen 2014). The late 1970s have been identified as a break point in the trend of glacial declines: mean mass balances per year were −0.2 m water equivalent (w.e.) between 1964 and 1975, and increased to −0.76 m w.e. between 1976 and 2010 (Rabatel et al. 2013). This timing coincides with a shift of the SAMS (Carvalho et al. 2011a, b).

It has been argued that monthly mass balance measurements on glaciers in Bolivia, Ecuador, and Colombia are controlled by the variability of sea surface temperatures of the Pacific Ocean at decadal time scales (Rabatel et al. 2013), but other climatic phenomena such as ENSO cycles or the Madden Julian Oscillation (MJO) (e.g., Carvalho et al. 2004) may have similar impacts. No clear precipitation trend has been identified in the tropical Andes, but temperature increased at a rate of 0.10 °C/decade during the last 70 years. It has been argued that more ENSO events with changing spatiotemporal patterns and a warming troposphere over the tropical Andes may explain much of the recent glacial shrinkage (Bradley et al. 2009, 2006; Hardy et al. 2003; Rabatel et al. 2013).

Glaciers in the northern central Andes span a wide range of elevations (Fig. 11.6), and the glacial retreat rate is dependent on glacial median elevation: glaciers with lower median elevation are declining at faster rates than those with higher median elevations. Specifically, glaciers with median elevations around 5.2 km asl are retreating at a rate of ~1 m $year^{-1}$ faster than glaciers with median elevations around 5.4 km asl (Hanshaw and Bookhagen 2014). To the south of the Peruvian Cordillera, glaciers in the Bolivian Cordillera Real have lost between 60 and 80 % of their mass since the mid-seventeenth to early eighteenth centuries, with most of the mass loss occuring during the past 50 years (Rabatel et al. 2013). The southernmost glaciers influenced by the monsoon are near 24°S (Fig. 11.4); the ubiquitous glaciers to the south are fed not only by the South American Monsoon System, but by the westerly wind systems and are not taken into account in this chapter.

Glacial retreat or advance is controlled by several factors, including precipitation, temperature, ice rheology, and surface-energy budgets. In tropical locations, temperature stays surprisingly similar throughout the year (Kaser 1999; Vuille et al. 2008) (cf. Fig. 11.5e), but overall temperature gradients vary (Fig. 11.6d). Daily temperatures throughout the year are fairly constant across 30° of latitude from north of the Equator to the south-central Andes (Fig. 11.5d, e). However, in the extra-tropical regions south of ~30°S, temperatures have a seasonal component and vary by more than 7.5 °C (Fig. 11.5e). The atmospheric lapse rate that describes the temperature change with elevation has a slightly negative trend from north to south but is generally constant along the tropical central Andes (Fig. 11.6d). Austral summer lapse rates (November to April) in the tropical Andes are between −6 and −7 °C/km, but increase to higher rates (~−4.5 °C/km) to the south in the extra-tropical regions. The austral winter atmospheric overall lapse rate is slightly higher, but shows similar spatial patterns to the austral summer lapse rate. The lapse rates at the latitudes of the central Andean plateau (Altiplano and Puna de Atacama) is higher than in the northern central Andes, because of a decrease of the temperature gradient between foreland and plateau region: the high-elevation Altiplano and Puna de Atacama orogenic plateaus heat up and reduce the temperature gradient (Fig. 11.6d). This phenomenon also has been observed in the Tibetan Plateau area (cf. Fig. 11.10c). The decrease in the atmospheric lapse rate in the central Andean plateau region leads to higher temperatures at higher elevations as compared to northern regions. This reduces the area that can be glacierized, and hence glacial areas in this region are smaller because of a decrease in moisture supply and higher temperatures.

Average daily temperatures and annual temperature variation have a strong topographic control: Intermontane basins that are lower than surrounding mountain ridges, for example, basins of 10–10,000 km^2 on the Altiplano-Puna de Atacama Plateau or in the south-central Andes, show larger annual temperature variation than the eastern slopes of the Andes (Fig. 11.5d, e). These intermontane basins influence local climate, lapse rates, and precipitation processes (Bookhagen and Strecker 2008; Rohrmann et al. in ~~review~~; Romatschke and Houze 2013). 2014

The occurrence of glaciers is controlled by moisture supply and temperature, and both factors are controlled by topography and the monsoon. Only the highest peaks are covered by glaciers (Fig. 11.5b) and only in regions with sufficient moisture supply and steep atmospheric lapse rates. The heavily glacierized eastern Cordillera in Peru receives large amounts of rainfall (Fig. 11.5b, c). But to the south of this area, present-day rainfall decreases and fewer current glaciers exist. During previous pluvial periods in the Late Pleistocene, these areas received more moisture in conjunction with a possible temperature decrease, and mountain peaks were glaciated (Abbott et al. 2003; Haselton et al. 2002). Thus, the central Andes centering around 20°S have large areas of more than 5 km elevation and can be glacierized, if atmospheric conditions allow.

11.4 Glaciers in the Himalayas and the Indian Monsoon System (IMS)

11.4.1 Climatic Background

Two principal climate regimes dominate High Mountain Asia (HMA): the Indian Summer Monsoon ~~(ISM)~~ and the Winter Western Disturbances (WWD). During the remove summer months, the monsoon is driven by a temperature differential between ocean and land, and upon encountering the orographic barrier of the Himalayas, monsoonal winds bring heavy precipitation to the region (see Chaps. 3 and 4). In the western part of the HMA, monsoonal precipitation is significantly less than in the east and central Himalayas, principally because of the increasing distance from the Bay of Bengal—the main source of water vapor for the monsoon (Bookhagen and Burbank 2006, 2010; Wulf et al. 2010).

During the winter, the pressure gradient that drives the monsoon reverses, resulting in WWD—westerly upper tropospheric synoptic-scale waves (Wulf et al. 2010). In contrast to the monsoons, WD travel at higher tropospheric altitudes and are therefore susceptible to orographic capture and intensification at high elevations (Lang and Barros 2004; Wulf et al. 2010). The WD are responsible for much of the winter precipitation in western HMA, especially at large-scale topographic features such as the Karakoram (Wulf et al. 2010). As a result, the western half of HMA receives more snowfall than the central or eastern Himalayas, demonstrated by the significantly greater snow-covered area (SCA) (Immerzeel et al. 2009; Wulf et al. 2010) (Fig. 11.9b). Consequently, snowmelt contributions to annual river runoff in western HMA are considerably greater in comparison to the eastern and central Himalayas, where monsoonal rainfall is the dominant source of river runoff (Immerzeel et al. 2009; Jeelani et al. 2012; Wulf et al. 2010) (Fig. 11.7).

In addition to the WD, the Tien Shan also experiences winter storms originating from the Siberian steppes (Aizen et al. 1995). The interaction between the WWD and the North Atlantic oscillation, as well as the Siberian anticyclonic circulation, determines the quantity of winter precipitation for the region, and this can vary along the entire mountain range (Aizen et al. 1997). Importantly, similar to the Himalayas, the northern Tien Shan experience a precipitation and mean temperature gradient that runs from the northwest to the southeast (Sorg et al. 2012).

Seasonal snow in HMA also plays an important role in the regional climate (Bookhagen and Burbank, 2010; Immerzeel et al. 2009; Wang et al. 2014) (Fig. 11.7). Upper tropospheric air temperatures over the Tibetan Plateau are

Layout: T1 Standard Unicode | Book ID: 314356_1_En | Book ISBN: 978-3-319-21649-2
Chapter No.: 11 | Date: 24-10-2015 | Time: 10:33 am | Page: 14/25

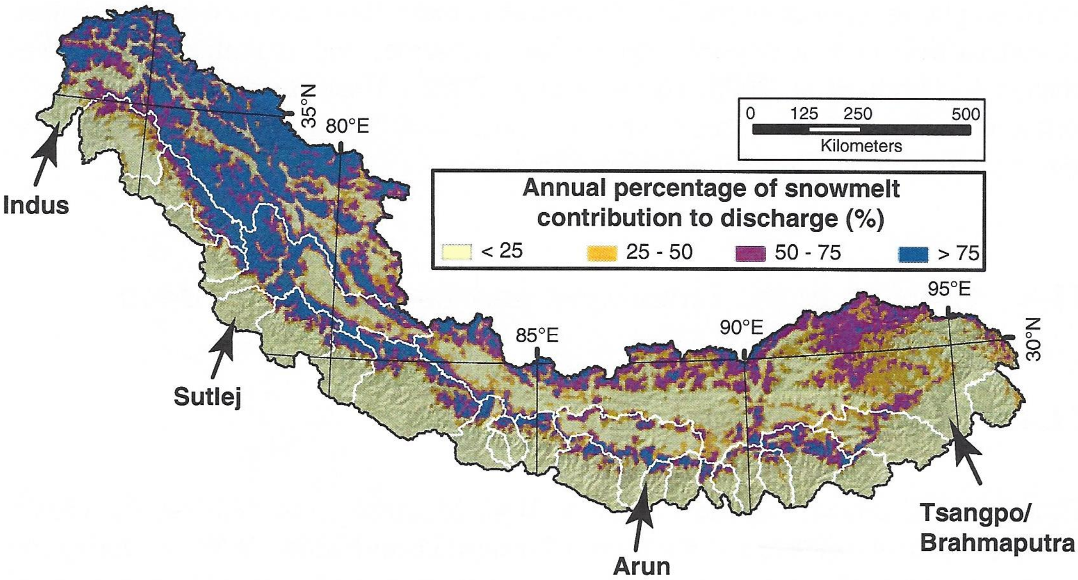

Fig. 11.7 The spatial pattern of snowmelt contribution to river discharge in the Himalayas derived from calibrated and validated satellite products and degree-day runoff modeling (modified according to Bookhagen and Burbank 2010). Note the high snowmelt contribution in the western Himalayas (e.g., the Indus and Sutlej catchments). Crucially, the areas with significant annual snowmelt contribution to river runoff are located at high elevations in remote regions with few to no monitoring stations

substantially warmer than air temperatures above the Indian Ocean. This tropospheric temperature gradient is thought to drive the Indian monsoon (Fu and Fletcher 1985). It has been hypothesized that larger amounts of seasonal snow cover over the Tibetan Plateau could reduce the magnitude of the Indian monsoon by reducing land surface temperatures, thereby reducing the tropospheric temperature gradient (Barnett et al. 1989; Blanford 1884). However, some recent studies indicate ~~have refuted this hypothesis, finding~~ a weak positive correlation between Eurasian snow cover and monsoon rainfall (Robock et al. 2003). While reductions in seasonal snow in western HMA may or may not affect monsoon rainfall, such reductions would seriously decrease water resource availability for river basins in the west.

The WD are responsible for much of the seasonal snow accumulation in HMA (Dimri 2005; Wulf et al. 2010) (Fig. 11.7). Still, the Indian summer monsoon can contribute high elevation seasonal snow to the central and eastern Himalayas and the Tibetan Plateau (Bookhagen and Burbank 2006; Bookhagen et al. 2005; Putkonen 2004; Wulf et al. 2010). However, SCA is more extensive and persistent in the western Himalayas than in the central and eastern Himalayas (Bookhagen and Burbank 2010), and also peaks much later in the western Himalayas (Immerzeel et al. 2009). Furthermore, snowlines are lower in the western Himalayas (Scherler et al. 2011a). These findings are consistent with the higher topography of the western Himalayas and the storm tracks of the WD. In general, snow cover has trended downward throughout HMA, but in some cases SCA has increased, for

Layout: T1 Standard Unicode | Book ID: 314356_1_En | Book ISBN: 978-3-319-21649-2
Chapter No.: 11 | Date: 24-10-2015 Time: 10:33 am | Page: 15/25

example in the Karakoram (Immerzeel et al. 2009; Tahir et al. 2011). This finding is consistent with the Karakoram glacier anomaly—a region of positive mass balance, either as a result of increased wintertime precipitation or decreased summer temperature (Bolch et al. 2012). Either way, it is important to note that in both Immerzeel et al. (2009) and Tahir et al. (2011), trends were not significant at the 0.05 confidence interval and the study time periods were relatively short, i.e., <10 years. In the Tien Shan and Hindu Kush, there is less information on the spatial and temporal extent of SCA. However, in the Tien Shan, snow cover thickness and duration have been found to be steadily decreasing since the 1940s (Aizen et al. 1997; Sorg et al. 2012).

11.4.2 Glacial Retreat Rates and Trends

The release of glacial melt reaches its crest in the summer and early autumn and can be critical for both agricultural activities and natural ecosystems (Alford and Armstrong 2010; Bolch et al. 2012; Ficke et al. 2007; Menon et al. 2013; Sorg et al. 2012; Sultana et al. 2009; Valentin et al. 2008; Wulf et al. 2010). As a result, changes in the melt water regime due to climate warming could have consequences for food security and ecosystem services, particularly for the western HMA. Melting glaciers can also increase the risk of ice/snow avalanches and glacial lake outburst floods (Quincey et al. 2007; Richardson and Reynolds 2000). However, it is unlikely that significant changes in annual runoff will occur soon, although shrinkage outside the Karakoram will increase the seasonality of runoff with impact on agriculture and hydropower generation. Glaciers in the western Himalayas are larger than in the central or eastern Himalayas, and thus will have a slower response time to climatic shifts (Fig. 11.8). AQ2

Most Himalayan glaciers are losing mass at rates similar to glaciers around the globe, except for the Karakoram area (Bolch et al. 2012; Gardelle et al. 2012; Kaab et al. 2012; Scherler et al. 2011b). Despite recent efforts, the climatic and cryospheric processes in the high-elevation Himalayas are still poorly understood. This is partly due to the difficultly inherent in accessing this region, but also due to the size and topographic complexity of glaciers in the region (Hewitt 2014). In western HMA, glaciers are in general receding, but not responding uniformly to climate warming (Hewitt 2014; Scherler et al. 2011b). Regional patterns have been detected, but even these have inconsistencies as a result of local variations in climate. Mayewski and Jeschke (1979) compiled the first observations of glacier advance and retreat in HMA. The study's database was spatially limited, but the "big picture" indicated that most glaciers were in retreat or standing still since about 1850. Current observations suggest that this trend is continuing in the central and eastern Himalayas and the outer Tien Shan (Bolch et al. 2012; Gardelle et al. 2012; Kaab et al. 2012; Scherler et al. 2011b; Sorg et al. 2012). However, the Karakoram has remained a regional anomaly (Bolch et al. 2012; Gardelle et al. 2013; Hewitt 2005); Karakoram glaciers have oscillated or surged over the past century, Color Scale missing!

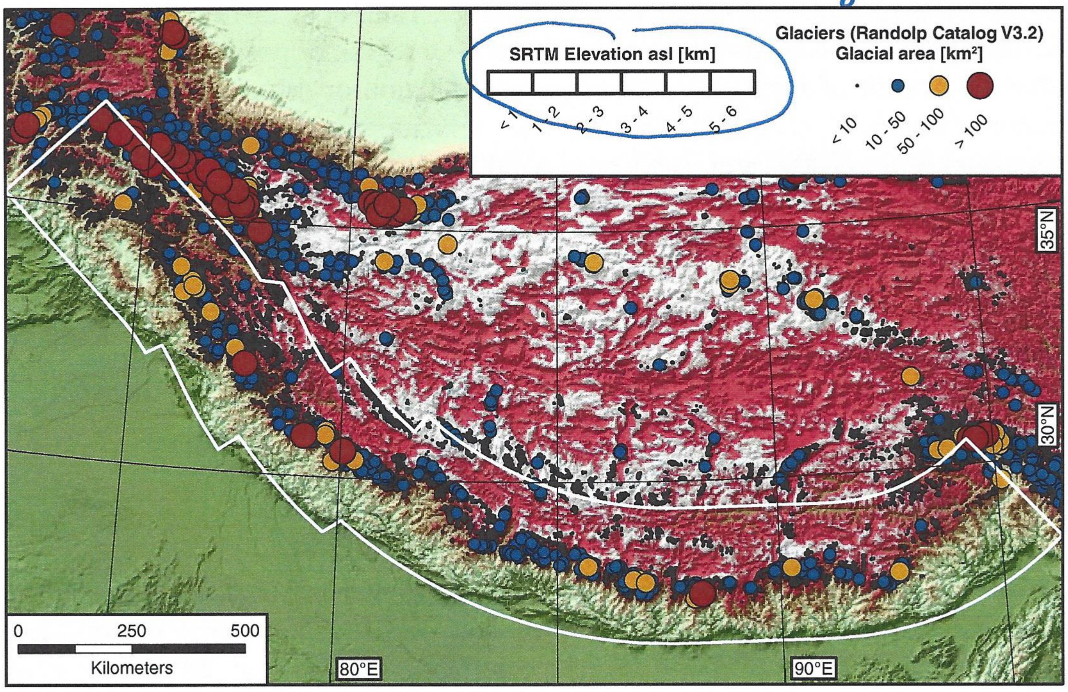

Fig. 11.8 SRTM topography and glacial sizes following the Randolph Catalog V3.2 (Arendt et al. 2012). The *white delineated area* following the main Himalayan arc indicates the area of the longitudinal profile shown in Fig. 11.10. Note the large glacial sizes in the western and northwestern Himalayas

indicating a positive mass balance. Recently, Gardelle et al. (2012) speculated that increased winter precipitation and/or cooler summers might be responsible for glacier stability or expansion in the Karakoram.

The depletion of many Himalayan glaciers has garnered media attention in recent years, because of concern over the future of regional water resources. However, while glacial melt may constitute most of the summer discharge in headwater basins, glacial melt over bigger watersheds comprises only a small amount of the annual river runoff (Bookhagen and Burbank 2010; Jeelani et al. 2012; Pal et al. 2013). For example, in the Liddar watershed (a tributary of the Indus), glacial melt contributes 2 % to the annual total, whereas snowmelt comprises 60 % of the annual runoff (Jeelani et al. 2012).

The glacial size distribution in the Himalayas shows a clear climatic and topographic signal (Fig. 11.9): glaciers in the western Himalayas receive significant precipitation in the form of snow during WD, resulting in significant snowcover (Fig. 11.9b) and snow-water amounts (Fig. 11.10b). In addition, the potential area that can be glaciated—for example, delineated by the area above 5 km elevation—is much larger in the western Himalayas than in the eastern (Fig. 11.10a). Mean annual temperatures in the western Himalayas are lower and also show a larger variability, based on daily temperature data collected during nighttime conditions from March 2001 until April 2014 (MODIS product MOD11C1 Wan 2008) (Fig. 11.9e, f). Rainfall in the Himalayan foreland shows a clear east-to-west

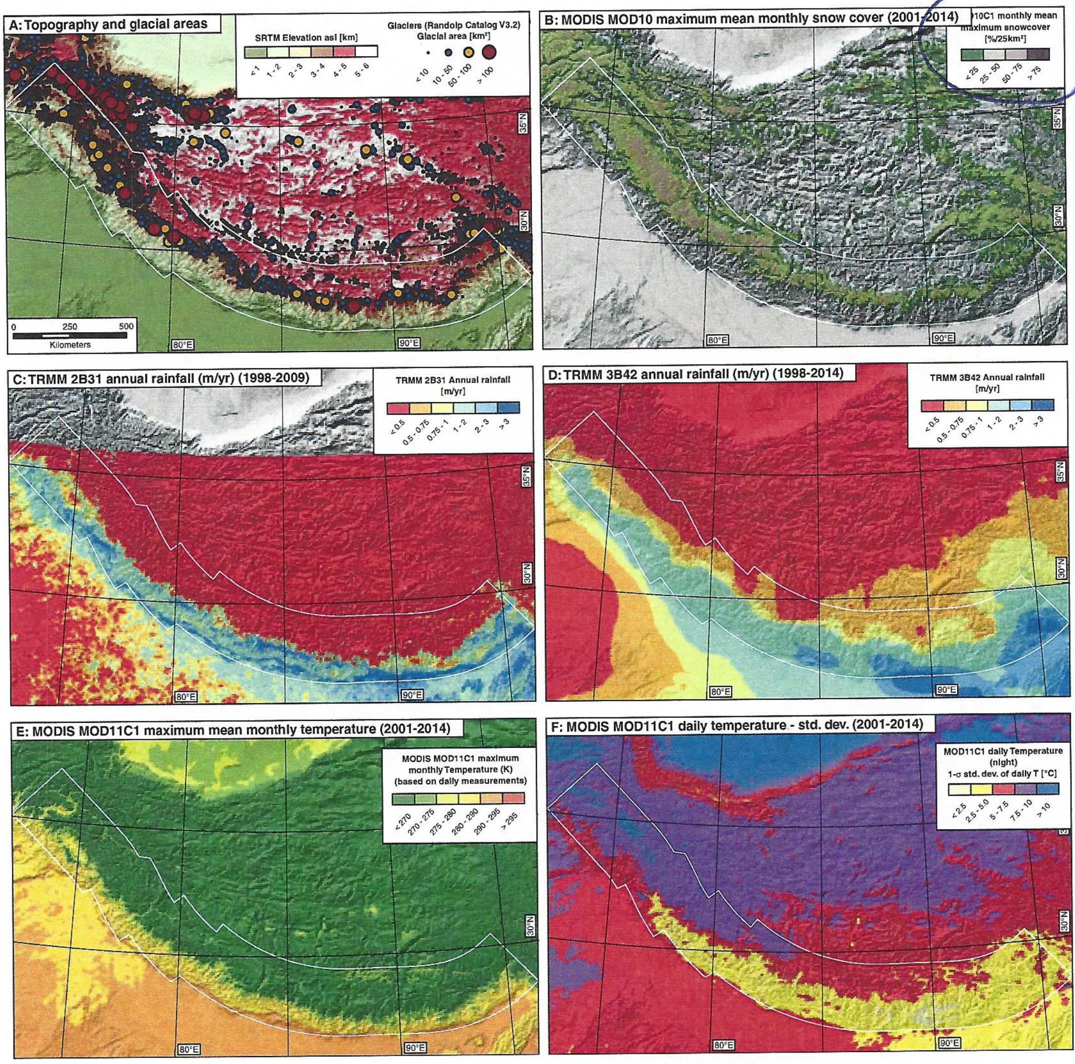

move legend down

Fig. 11.9 Dataset compilation for the Himalayas. **a** Shows SRTM topography and glacier locations based on RGI V3.2 (Arendt et al. 2012). **b** MODIS MOD10C1 maximum mean monthly snowcover based on daily data from March 2001 to April 2014 (Hall et al. 2006). There is a steep east-to-west snow cover gradient with high snowcover amounts in the western Himalayas due to heavy snowfall during westerly disturbances. **c** Mean annual rainfall based on high-spatial resolution TRMM 2B31 data (Bookhagen and Burbank 2006, 2010; Bookhagen and Strecker 2008). There is a band of nearly continuous, high orographic rainfall at the first topographic rise of the Himalayas—separating the Ganges Plain from the mountainous Himalayas. **d** Mean annual TRMM3B42 rainfall (spatial resolution: $\sim 25 \times 25$ km^2 and 3-h temporal resolution) (Boers et al. 2013; Bookhagen and Strecker 2010; Huffman et al. 2007). Note the overall similarity between TRMM3B42 and 2B31 rainfall patterns, but only the TRMM 2B31 data depict the orographic rainfall band. **e** MODIS MOD11C1 maximum mean monthly temperature based on daily data from March 2001 to April 2014 collected during nighttime conditions (Wan 2008). **f** 1-sigma standard deviation of daily temperature (nighttime conditions) from March 2001 to April 2014. Note the low-to-moderate variability in the eastern and central Himalayas, but the high variability in the western Himalayas and in the southern Tibetan Plateau

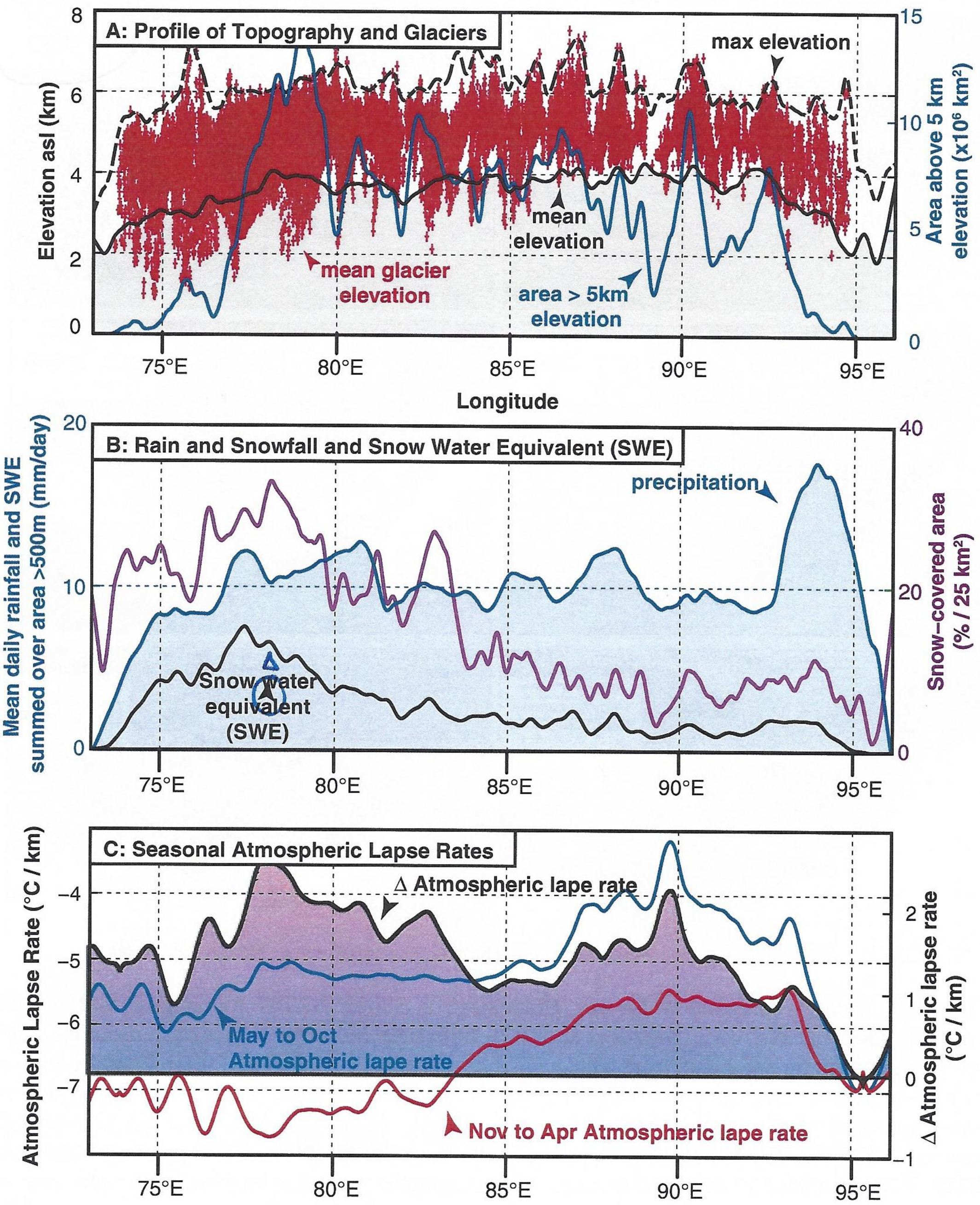

move arrowhead up

Fig. 11.10 West-to-east profiles showing topography, climatic variables, and atmospheric lapse rates. Values have been averaged from north to south within the *white delineated area* shown in Figs. 11.8 and 11.9. **a** Maximum (*black, dashed line*) and mean elevation (*solid line*) and area above 5-km elevation. Note the different Y-axis scales as compared to Fig. 11.6. *Red crosses* denote mean glacier elevation. **b** TRMM 3B42-derived precipitation is shown in *blue* and snow-water equivalent (SWE) in *black* (both datasets are shown with the same Y-axis scale). The *magenta line* denotes a snow-covered area. Note the west-to-east gradient with high snow cover in the western areas due to the influence of winter westerly disturbance. **c** Summer atmospheric lapse rates (*blue line*) are higher than during the winter (*red line*). Lapse rates in the central and eastern Himalayas are higher in the summertime (i.e., higher temperatures at higher elevations) because of the heating of the Tibetan Plateau and a reduction of the temperature gradient

Layout: T1 Standard Unicode | Book ID: 314356_1_En | Book ISBN: 978-3-319-21649-2
Chapter No.: 11 | Date: 24-10-2015 | Time: 10:33 am | Page: 19/25

gradient with more rainfall in the eastern regions closer to the moisture source of the Bay of Bengal (Bookhagen and Burbank 2010) (Fig. 11.9c, d). However, rainfall in the mountainous Himalayas is more evenly distributed and doesn't show a strong gradient, although rainfall to the west of the Shillong Plateau at 90E is higher than elsewhere in the Himalayas (Figs. 11.9c, d and 11.10b) (Bookhagen and Burbank 2010; Bookhagen et al. 2005).

In order to decipher the large-scale climatic and topographic gradients and their impact on glaciers, a west-to-east profile was constructed that averages values along the Himalayan arc in a north–south direction (Fig. 11.10). I focus on the areas above 500 m elevations and exclude low-elevation areas such as the Ganges foreland and Indus plain. In other words, the focus is on data close to the main Himalayan arc and does not include the Tibetan plateau. The area is outlined by a white polygon in Figs. 11.9 and 11.10. This analysis reveals that the maximum elevations along the Himalayan arc remain roughly similar and vary between 6 and 8 km (Fig. 11.10a), but the area above 5 km varies widely and hence modifies conditions for cryospheric processes. These data are an approximation of the hypsometric differences between the eastern and western Himalayas. A clear west-to-east gradient exists for snow-covered areas and snow-water equivalent with large amounts of both in the west. There, about half of the annual precipitation falls as snow (Fig. 11.10b). The summer atmospheric lapse rate is between 5–6 °C/km in the western and central Himalayas, but decreases to 3.5–4.5 °C/km in the eastern Himalayas due to a stronger heating of the Tibetan Plateau (Fig. 11.10c); this is significant because higher elevations in the eastern Himalayas tend to be warmer than in the western. The winter atmospheric lapse rate shows a weaker west-to-east gradient because of reduced impacts of the high-elevation Tibetan Plateau.

11.5 Conclusions

Two areas of the global monsoonal domain are characterized by significant glaciation: the northern and central Andes and the Himalayas (cf. Fig. 11.1). This chapter elucidates the differences in climatic and topographic boundary conditions between the two. The tropical northern and central Andes have no seasonal snow cover, and glaciers of small to moderate size are limited to high-elevation areas. In contrast, the western Himalayas have a significant winter snow cover due to the influence of "Winter ~~Western~~ Disturbances," and this area hosts some of the largest glaciers outside of the polar regions and Greenland (Fig. 11.8). While precipitation and seasonal moisture distribution is important for glacier occurrence, hypsometry (or "area vs. elevation") can have significant impacts as well. The central Himalayas and the Cordillera Blanca in Peru do not provide large accumulation areas at high elevations and hence glaciers are limited to the relatively small areas at which year-round temperatures are low and moisture supply is sufficient. The western Himalayas have large areas above 5 and 6 km elevation (Fig. 11.10c). At decadal or longer time scales, the atmospheric lapse rate or temperature changes with elevation

Ok! no changes
~~Westerly~~

influence glacial behavior. It is important to note that an annual lapse rate may not be representative of the relevant conditions influencing glacial formation, and instead, seasonal lapse rates are more useful for deciphering temperature changes with elevation (Figs. 11.6c and 11.10c).

References

Abbott MB, Wolfe BB, Wolfe AP, Seltzer GO, Aravena R, Mark BG, Polissar PJ, Rodbell DT, Rowe HD, Vuille M (2003) Holocene paleohydrology and glacial history of the central Andes using multiproxy lake sediment studies. Palaeogeogr Palaeoclimatol Palaeoecol 194(1–3):123–138. doi:10.1016/s0031-0182(03)00274-8

Aizen VB, Aizen EM, Melack JM (1995) Climate, snow cover, glaciers, and runoff in the Tien-Shan, Central-Asia. Water Resour Bull 31(6):1113–1129

Aizen VB, Aizen EM, Melack JM, Dozier J (1997) Climatic and hydrologic changes in the Tien Shan, Central Asia. J Clim 10(6):1393–1404. doi:10.1175/1520-0442(1997)010<1393:cahcit>2.0.co;2

Alford D, Armstrong R (2010) The role of glaciers in stream flow from the Nepal Himalaya. Cryosphere Discuss 4(2):469–494. doi:10.5194/tcd-4-469-2010

Andermann C, Bonnet S, Gloaguen R (2011) Evaluation of precipitation data sets along the Himalayan front, *Geochemistry Geophysics Geosystems*, *12*, doi:10.1029/2011gc003513

Archer DR, Fowler HJ (2004) Spatial and temporal variations in precipitation in the Upper Indus Basin, global teleconnections and hydrological implications. Hydrol Earth Syst Sci 8(1):47–61

Arendt A et al (2012) Randolph glacier inventory—a dataset of global glacier outlines: Version 3.2, edited, Global Land Ice Measurements from Space, Boulder, Colorado, USA. Digital Media

Baraer M, Mark BG, McKenzie JM, Condom T, Bury J, Huh KI, Portocarrero C, Gomez J, Rathay S (2012) Glacier recession and water resources in Peru's Cordillera Blanca. J Glaciol 58(207):134–150. doi:10.3189/2012JoG11J186

Barnett TP, Adam JC, Lettenmaier DP (2005) Potential impacts of a warming climate on water availability in snow-dominated regions. Nature 438(7066):303–309. doi:10.1038/nature04141

Barnett TP, Dümenil L, Schlese U, Roeckner E, Latif M (1989) The effect of Eurasian snow cover on regional and global climate variations. J Atmos Sci 46(5):661–686. doi:10.1175/1520-0469(1989)046<0661:TEOESC>2.0.CO;2

Blanford HF (1884) On the connexion of the Himalaya snowfall with dry winds and seasons of drought in India. Proc R Soc London 37:1–23

Boers N, Bookhagen B, Marwan N, Kurths J, Marengo J (2013) Complex networks identify spatial patterns of extreme rainfall events of the South American Monsoon System. Geophys Res Lett 40(16):4386–4392. doi:10.1002/grl.50681

Bolch T et al (2012) The state and fate of Himalayan glaciers. Science 336(6079):310–314. doi:10.1126/science.1215828

Bolch T, Pieczonka T, Benn DI (2011) Multi-decadal mass loss of glaciers in the Everest area (Nepal Himalaya) derived from stereo imagery. Cryosphere 5(2):349–358. doi:10.5194/tc-5-349-2011

Bookhagen B (2010) Appearance of extreme monsoonal rainfall events and their impact on erosion in the Himalaya. Geomat Nat Hazards Risk 1(1):37–50. doi:10.1080/19475701003625737

Bookhagen B, Burbank DW (2006) Topography, relief, and TRMM-derived rainfall variations along the Himalaya. Geophys Res Lett 33(8). doi:10.1029/2006gl026037

Bookhagen B, Burbank DW (2010) Toward a complete Himalayan hydrological budget: spatiotemporal distribution of snowmelt and rainfall and their impact on river discharge. J Geophys Res Earth Surf 115. doi:10.1029/2009jf001426

Bookhagen B, Strecker MR (2008) Orographic barriers, high-resolution TRMM rainfall, and relief variations along the eastern Andes. Geophys Res Lett 35(6). doi:10.1029/2007gl032011

Bookhagen B, Strecker MR (2010) Modern Andean rainfall variation during ENSO cycles and its impact on the Amazon Basin. In: Hoorn HVC, Wesselingh F (eds) Neogene history of Western Amazonia and its significance for modern diversity. Blackwell Publishing, Oxford

Bookhagen B, Strecker MR (2012) Spatiotemporal trends in erosion rates across a pronounced rainfall gradient: Examples from the southern Central Andes. Earth Planet Sci Lett 327:97–110. doi:10.1016/j.epsl.2012.02.005

Bookhagen B, Thiede RC, Strecker MR (2005) Abnormal monsoon years and their control on erosion and sediment flux in the high, and northwest Himalaya. Earth Planet Sci Lett 231(1–2):131–146. doi:10.1016/j.epsl.2004.11.014

Bradley RS, Keimig FT, Diaz HF, Hardy DR (2009) Recent changes in freezing level heights in the Tropics with implications for the deglacierization of high mountain regions. Geophys Res Lett 36. doi:10.1029/2009gl037712

Bradley RS, Vuille M, Diaz HF, Vergara W (2006) Threats to water supplies in the tropical Andes. Science 312(5781):1755–1756. doi:10.1126/science.1128087

Buytaert W, Celleri R, De Bievre B, Cisneros F, Wyseure G, Deckers J, Hofstede R (2006) Human impact on the hydrology of the Andean paramos. Earth Sci Rev 79(1–2):53–72. doi:10.1016/j.earscirev.2006.06.002

Buytaert W, Cuesta-Camacho F, Tobon C (2011) Potential impacts of climate change on the environmental services of humid tropical alpine regions. Glob Ecol Biogeogr 20(1):19–33. doi:10.1111/j.1466-8238.2010.00585.x

Buytaert W, De Bievre B (2012) Water for cities: the impact of climate change and demographic growth in the tropical Andes. Water Resour Res 48. doi:10.1029/2011wr011755

Carvalho LMV, Jones C, Liebmann B (2002) Extreme precipitation events in southeastern South America and large-scale convective patterns in the South Atlantic convergence zone. J Clim 15(17):2377–2394. doi:10.1175/1520-0442(2002)015<2377:epeiss>2.0.co;2

Carvalho LMV, Jones C, Liebmann B (2004) The South Atlantic convergence zone: Intensity, form, persistence, and relationships with intraseasonal to interannual activity and extreme rainfall. J Clim 17(1):88–108. doi:10.1175/1520-0442(2004)017<0088:tsaczi>2.0.co;2

Carvalho LMV, Jones C, Posadas AND, Quiroz R, Bookhagen B, Liebmann B (2012) Precipitation characteristics of the South American Monsoon System derived from multiple datasets. J Clim 25(13):4600–4620. doi:10.1175/jcli-d-11-00335.1

Carvalho LMV, Jones C, Silva AE, Liebmann B, Dias PLS (2011a) The South American Monsoon System and the 1970s climate transition. Int J Climatol 31(8):1248–1256. doi:10.1002/joc.2147

Carvalho LMV, Silva AE, Jones C, Liebmann B, Dias PLS, Rocha HR (2011b) Moisture transport and intraseasonal variability in the South America monsoon system. Clim Dyn 36(9–10):1865–1880. doi:10.1007/s00382-010-0806-2

Dimri AP (2005) The contrasting features of winter circulation during surplus and deficient precipitation over Western Himalayas. Pure appl Geophys 162(11):2215–2237. doi:10.1007/s00024-006-0092-4

Farr TG et al (2007) The shuttle radar topography mission. Rev of Geophys 45(2). doi:10.1029/2005rg000183

Ficke AD, Myrick CA, Hansen LJ (2007) Potential impacts of global climate change on freshwater fisheries. Rev Fish Biol Fish 17(4):581–613. doi:10.1007/s11160-007-9059-5

Finger D, Heinrich G, Gobiet A, Bauder A (2012) Projections of future water resources and their uncertainty in a glacierized catchment in the Swiss Alps and the subsequent effects on hydropower production during the 21st century. Water Resour Res 48, W02521. doi:10.1029/2011wr010733

Francou B, Vuille M, Wagnon P, Mendoza J, Sicart JE (2003) Tropical climate change recorded by a glacier in the central Andes during the last decades of the twentieth century: Chacaltaya, Bolivia, 16 degrees S. J Geophys Res Atmos 108(D5). doi:10.1029/2002jd002959

Fu C, Fletcher JO (1985) The relationship between Tibet-tropical ocean thermal contrast and interannual variability of Indian monsoon rainfall. J Climate Appl Meteorol 24(8):841–847. doi:10.1175/1520-0450(1985)024<0841:TRBTTO>2.0.CO;2

Gardelle J, Berthier E, Arnaud Y (2012) Slight mass gain of Karakoram glaciers in the early twenty-first century. Nat Geosci 5(5):322–325. doi:10.1038/ngeo1450

Gardelle J, Berthier E, Arnaud Y, Kaab A (2013) Region-wide glacier mass balances over the Pamir-Karakoram-Himalaya during 1999-2011. Cryosphere 7(4):1263–1286. doi:10.5194/tc-7-1263-2013

Hall DK, Riggs GA, Salomonson VV (2006) MODIS/Terra snow cover daily L3 global 0.05 deg CMG V005, MOD10C1, Digital Media, edited, National Snow and Ice Data Center, Boulder, Colorado USA

Hanshaw MN, Bookhagen B (2014) Glacial areas, lake areas, and snow lines from 1975 to 2012: status of the Cordillera Vilcanota, including the Quelccaya Ice Cap, northern central Andes, Peru. The Cryosphere 8(2):359–376. doi:10.5194/tc-8-359-2014

Hardy DR, Vuille M, Bradley RS (2003) Variability of snow accumulation and isotopic composition on Nevado Sajama, Bolivia. J Geophys Res Atmos 108(D22). doi:10.1029/2003jd003623

Haselton K, Hilley G, Strecker MR (2002) Average Pleistocene climatic patterns in the southern central Andes: controls on mountain glaciation and paleoclimate implications. J Geol 110 (2):211–226. doi:10.1086/338414

Hewitt K (2005) The Karakoram anomaly? Glacier expansion and the 'elevation effect', Karakoram Himalaya. Mt Res Dev 25(4):332–340. doi:10.1659/0276-4741(2005)025[0332:tkagea]2.0.co;2

Hewitt K (2014) Glaciers of the Karakoram Himalaya. Springer, Dordrecht

Huffman GJ, Adler RF, Bolvin DT, Gu GJ, Nelkin EJ, Bowman KP, Hong Y, Stocker EF, Wolff DB (2007) The TRMM multisatellite precipitation analysis (TMPA): quasi-global, multiyear, combined-sensor precipitation estimates at fine scales. J Hydrometeorol 8(1):38–55. doi:10.1175/jhm560.1

Huggel C, Kaab A, Haeberli W, Teysseire P, Paul F (2002) Remote sensing based assessment of hazards from glacier lake outbursts: a case study in the Swiss Alps. Can Geotech J 39(2):316–330. doi:10.1139/t01-099

Huss M (2012) Extrapolating glacier mass balance to the mountain range scale: the European Alps 1900-2100. Cryosphere Discuss 6(1117–1156)

Huss M, Farinotti D, Bauder A, Funk M (2008) Modelling runoff from highly glacierized alpine drainage basins in a changing climate. Hydrol Process 22(19):3888–3902. doi:10.1002/hyp.7055

Immerzeel WW, Droogers P, de Jong SM, Bierkens MFP (2009) Large-scale monitoring of snow cover and runoff simulation in Himalayan river basins using remote sensing. Remote Sens Environ 113(1):40–49. doi:10.1016/j.rse.2008.08.010

IPCC (2013) Climate change 2013: the physical science basis. Contribution of Working Group I to the fifth assessment report of the intergovernmental panel on climate change. Cambridge University Press, Cambridge, United Kingdom and New York, NY, USA, 1535 pp

Jacob T, Wahr J, Pfeffer WT, Swenson S (2012) Recent contributions of glaciers and ice caps to sea level rise. Nature 482(7386):514–518. doi:10.1038/nature10847

Jeelani G, Feddema JJ, van der Veen CJ, Stearns L (2012) Role of snow and glacier melt in controlling river hydrology in Liddar watershed (western Himalaya) under current and future climate. Water Resour Res 48. doi:10.1029/2011wr011590

Jones C, Carvalho LMV (2002) Active and break phases in the South American Monsoon System. J Clim 15(8):905–914. doi:10.1175/1520-0442(2002)015<0905:aabpit>2.0.co;2

Kaab A, Berthier E, Nuth C, Gardelle J, Arnaud Y (2012) Contrasting patterns of early twenty-first-century glacier mass change in the Himalayas. Nature 488(7412):495–498. doi:10.1038/nature11324

Kaser G (1999) A review of the modern fluctuations of tropical glaciers. Global Planet Change 22 (1–4):93–103. doi:10.1016/s0921-8181(99)00028-4

Kaser G (2001) Glacier-climate interaction at low latitudes. J Glaciol 47(157):195–204. doi:10.3189/172756501781832296

Kaser G, Cogley JG, Dyurgerov MB, Meier MF, Ohmura A (2006) Mass balance of glaciers and ice caps: consensus estimates for 1961-2004. Geophys Res Lett 33(19). doi:10.1029/2006gl027511

Kaser G, Grosshauser M, Marzeion B (2010) Contribution potential of glaciers to water availability in different climate regimes. Proc Natl Acad Sci USA 107(47):20223–20227. doi:10.1073/pnas.1008162107

Kitoh A, Endo H, Krishna Kumar K, Cavalcanti IFA, Goswami P, Zhou T (2013) Monsoons in a changing world: a regional perspective in a global context. J Geophys Res Atmos n/a–n/a. doi:10.1002/jgrd.50258

Lang TJ, Barros AP (2004) Winter storms in the central Himalayas. J Meteorol Soc Jpn 82(3):829–844. doi:10.2151/jmsj.2004.829

Lemke P et al (2007) Observations: changes in snow, ice and frozen ground, in climate change 2007: the physical science basis. In: Solomon S, Qin D, Manning M, Chen Z, Marquis M, Averyt KB, Tignor M, Miller HL (eds) Contribution of Working Group I to the fourth assessment report of the intergovernmental panel on climate change. Cambridge University Press, Cambridge, UK, pp 337–383

Marengo JA et al (2012) Recent developments on the South American Monsoon System. Int J Climatol 32(1):1–21. doi:10.1002/joc.2254

Mayewski PA, Jeschke PA (1979) Himalayan and Trans-Himalayan glacier fluctuations since AD 1812. Arct Alpine Res 267–287

Menon A, Levermann A, Schewe J (2013) Enhanced future variability during India's rainy season. Geophys Res Lett 40(12):3242–3247. doi:10.1002/grl.50583

Oerlemans J (2005) Extracting a climate signal from 169 Glacier records. Science 308(5722):675–677. doi:10.1126/science.1107046

Pal I, Lall U, Robertson AW, Cane MA, Bansal R (2013) Predictability of Western Himalayan river flow: melt seasonal inflow into Bhakra Reservoir in northern India. Hydrol Earth Syst Sci 17(6):2131–2146. doi:10.5194/hess-17-2131-2013

Paul F, Kaab A, Maisch M, Kellenberger T, Haeberli W (2004) Rapid disintegration of Alpine glaciers observed with satellite data. Geophys Res Lett 31(21). doi:10.1029/2004gl020816

Price MF, Weingartner R (2012) Global change and the world's mountains. Mt Res Dev 32(S1): S3–S6

Pulliainen J, Hallikainen M (2001) Retrieval of regional snow water equivalent from space-borne passive microwave observations. Remote Sens Environ 75(1):76–85. doi:10.1016/s0034-4257(00)00157-7

Putkonen JK (2004) Continuous snow and rain data at 500 to 4400 m altitude near Annapurna, Nepal, 1999-2001. Arct Antarct Alp Res 36(2):244–248. doi:10.1657/1523-0430(2004)036[0244:CSARDA]2.0.CO;2

Quincey DJ, Richardson SD, Luckman A, Lucas RM, Reynolds JM, Hambrey MJ, Glasser NF (2007) Early recognition of glacial lake hazards in the Himalaya using remote sensing datasets. Global Planet Change 56(1–2):137–152. doi:10.1016/j.gloplacha.2006.07.013

Rabatel A et al (2013) Current state of glaciers in the tropical Andes: a multi-century perspective on glacier evolution and climate change. Cryosphere 7(1):81–102. doi:10.5194/tc-7-81-2013

Radic V, Hock R (2011) Regionally differentiated contribution of mountain glaciers and ice caps to future sea-level rise. Nat Geosci 4(2):91–94. doi:http://www.nature.com/ngeo/journal/v4/n2/abs/ngeo1052.html-supplementary-information

Richardson SD, Reynolds JM (2000) An overview of glacial hazards in the Himalayas. Quatern Int 65:31–47

Robock A, Mu M, Vinnikov K, Robinson D (2003) Land surface conditions over Eurasia and Indian summer monsoon rainfall. J Geophys Res 108(D4):4131. doi:10.1029/2002JD002286

Rohrmann A, Strecker MR, Bookhagen B, Mulch A, Sachse D, Pingel H, Alonso RN, Schildgen TF, Montero C ~~(in review)~~ ~~Andean convective storms overprint isotope systematics in rainfall.~~ Earth Planet Sci Lett 2014

Romatschke U, Houze RA (2013) Characteristics of precipitating convective systems accounting for the summer rainfall of tropical and subtropical South America. J Hydrometeorol 14(1):25–46. doi:10.1175/jhm-d-12-060.1

Scherler D, Bookhagen B, Strecker MR (2011a) Hillslope-glacier coupling: the interplay of topography and glacial dynamics in High Asia. J Geophys Res Earth Surf 116. doi:10.1029/2010jf001751

Scherler D, Bookhagen B, Strecker MR (2011b) Spatially variable response of Himalayan glaciers to climate change affected by debris cover. Nat Geosci 4(3):156–159. doi:10.1038/ngeo1068

Sorg A, Bolch T, Stoffel M, Solomina O, Beniston M (2012) Climate change impacts on glaciers and runoff in Tien Shan (Central Asia). Nat Clim Change 2(10):725–731. doi:10.1038/NCLIMATE1592

Sultana H, Ali N, Iqbal MM, Khan AM (2009) Vulnerability and adaptability of wheat production in different climatic zones of Pakistan under climate change scenarios. Clim Change 94(1–2):123–142. doi:10.1007/s10584-009-9559-5

Tahir A, Chevallier P, Arnaud Y, Ahmad B (2011) Snow cover dynamics and hydrological regime of the Hunza River basin, Karakoram Range, Northern Pakistan. Hydrol Earth Syst Sci Discuss 8(2):2821–2860. doi:10.5194/hess-15-2275-2011

Tait AB (1998) Estimation of snow water equivalent using passive microwave radiation data. Remote Sens Environ 64(3):286–291. doi:10.1016/s0034-4257(98)00005-4

Tedesco M, Kelly R, Foster JL, Chang ATC (2004a) AMSR-E/Aqua Daily L3 global snow water equivalent EASE-grids. Version 2. [indicate subset used], edited, NASA DAAC at the National Snow and Ice Data Center, Boulder, Colorado USA

Tedesco M, Pulliainen J, Takala M, Hallikainen M, Pampaloni P (2004b) Artificial neural network-based techniques for the retrieval of SWE and snow depth from SSM/I data. Remote Sens Environ 90(1):76–85. doi:10.1016/j.rse.2003.12.002

Thompson LG, Mosley-Thompson E, Davis ME, Lin PN, Henderson K, Mashiotta TA (2003) Tropical glacier and ice core evidence of climate change on annual to millennial time scales. Clim Change 59(1–2):137–155. doi:10.1023/a:1024472313775

Valentin C et al (2008) Runoff and sediment losses from 27 upland catchments in Southeast Asia: Impact of rapid land use changes and conservation practices. Agric Ecosyst Environ 128(4):225–238. doi:10.1016/j.agee.2008.06.004

Vaughan DG et al (2013) Observations: cryosphere. In: Climate change 2013: the physical science basis. Contribution of Working Group I to the fifth assessment report of the intergovernmental panel on climate change. Cambridge University Press, Cambridge, United Kingdom and New York, NY, USA

Vera C et al (2006) Toward a unified view of the American monsoon systems. J Clim 19(20):4977–5000. doi:10.1175/jcli3896.1

Viviroli D, Weingartner R (2004) The hydrological significance of mountains: from regional to global scale. Hydrol Earth Syst Sci 8(6):1016–1029

Vuille M, Francou B, Wagnon P, Juen I, Kaser G, Mark BG, Bradley RS (2008) Climate change and tropical Andean glaciers: past, present and future. Earth Sci Rev 89(3–4):79–96. doi:10.1016/j.earscirev.2008.04.002

Wagnon P, Ribstein P, Francou B, Sicart JE (2001) Anomalous heat and mass budget of Glaciar Zongo, Bolivia, during the 1997/98 El Nino year. J Glaciol 47(156):21–28. doi:10.3189/172756501781832593

Wagnon P, Ribstein P, Kaser G, Berton P (1999) Energy balance and runoff seasonality of a Bolivian glacier. Global Planet Change 22(1–4):49–58. doi:10.1016/s0921-8181(99)00025-9

Rohrmann, A et al: Can stable isotopes ride out the storms? The role of convection for water isotopes in models, records, and paleoaltimetry studies in the central Andes, Earth Planet Sci Letters, 407, 187-195. doi: 10.1016/j.epsl.2014.09.021